

1 **Dual Targeting Nanoparticles for Epilepsy Therapy**

2 *Qinghong Hou*^{a, b, c‡}, *Lulu Wang*^{d‡}, *Feng Xiao*^a, *Le Wang*^a, *Xiaoyan Liu*^a, *Lina Zhu*
3 *c*, *Yi Lu*^{*d}, *Wenfu Zheng*^{*b}, *Xingyu Jiang*^{*a}

4

5 ^a Qinghong Hou, Feng Xiao, Le Wang, Xiaoyan Liu, Prof. Xingyu Jiang

6 **Shenzhen Key Laboratory of Smart Healthcare Engineering, Guangdong Provincial**
7 **Key Laboratory of Advanced Biomaterials, Department of Biomedical Engineering,**
8 **Southern University of Science and Technology, Shenzhen 518055, P. R. China.**

9 **E-mail: jiang@sustech.edu.cn.**

10 ^b Qinghong Hou, Prof. Wenfu Zheng

11 CAS Key Laboratory for Biomedical Effects of Nanomaterials and Nanosafety,
12 National Center for NanoScience and Technology, Beijing 100190, P. R. China

13 E-mail: zhengwf@nanoctr.cn

14 ^c Qinghong Hou, Prof. Lina Zhu

15 Department of Chemistry, School of Science, Tianjin University, Tianjin 300350, P.
16 R. China

17 ^d Lulu Wang, Prof. Yi Lu

18 CAS Key Laboratory of Brain Connectome and Manipulation, the Brain Cognition
19 and Brain Disease Institute, Shenzhen Institute of Advanced Technology, Chinese
20 Academy of Sciences; Shenzhen-Hong Kong Institute of Brain Science-Shenzhen
21 Fundamental Research Institutions, Shenzhen 518055, P. R. China.

22 E-mail: luyi@siat.ac.cn

23

24 **Experimental Methods**

25 **Materials**

26 PLGA (lactide:glycolide = 75:25) was from Evonik Industries (Germany). 1,2-
27 Dihexadecanoylrac-glycero-3-phosphocholine (DPPC), cholesterol, distearoyl
28 phosphoethanolamine (DSPE)-polyethylene glycol (PEG) 2k, and DSPE-PEG2k-Mal

29 were from Avanti Polar lipids (USA). Dimethylformamide, trifluoroethanol,
30 lamotrigine, pilocarpine hydrochloride, and urethane were from Aladdin.
31 Neurobasal medium, B27 supplement, penicillin/streptomycin (PS), F12/DMEM
32 medium, FBS and 1×PBS (and 10×PBS) were from Gibco. DiR was from Invitrogen.
33 DAPI and kainic acid (KA) monohydrate were from Sigma. Cell viability test kit and
34 DiI were from Shenzhen Kailian Biotechnology Co., Ltd. GFAP was from Abcam.
35 NeuN was from Millipore. Alexa Fluor 594 affipure goat anti-rabbit IgG (H_lL) and
36 Alexa Fluor 488 affipure goat anti-rabbit IgG (H_lL) were from Jackson
37 ImmunoResearch.

38 **Synthesis of DSPE-PEG2k-D-T7 and DSPE-PEG2k-Tet1**

39 DSPE-PEG2k-D-T7 was synthesized by conjugating DSPE-PEG2k-Mal to a cysteine
40 conjugated on D-T7 peptide (D-T7-Cys). Briefly, D-T7-Cys reacted with DSPE-
41 PEG2k-Mal (5:1 molar ratio) at RT under mild shaking for 24 h in PBS (Na₂HPO₄
42 and EDTA, pH = 7.2). The unreacted D-T7 peptides and the salts in the reaction
43 system were removed by an Amicon Ultra-4 ultrafilter (MWCO = 3KD, Millipore).
44 The DSPE-PEG2k-Tet1 was prepared in the same way. The final solution was freeze-
45 dried and stored at -20 °C until further use. Liquid chromatography-quadrupole
46 orbitrap mass spectrometer (LC-MS, Q Exactive) of DSPE-PEG2k-Mal, D-T7-Cys,
47 Tet1-Cys and DSPE-PEG2k-D-T7, DSPE-PEG2k-Tet1 were performed to confirm
48 the successful synthesis.

49 **Preparation and characterization of lipids@PL NPs with different surface** 50 **coatings**

51 The design and fabrication method of the microfluidic chip was the same as the
52 previous work.¹ In short, the microfluidic chip consisted of two stages, the first stage
53 consisted of three liquid inlets and a straight reaction channel. The second stage
54 consisted of a central liquid inlet and a spiral mixing channel. The three inlet channels
55 of the first stage were 100 μm wide and 60 μm high. The width and height of the

56 central liquid inlet channel and the spiral mixing channel of the second stage was 300
57 μm and 60 μm respectively ². We synthesized LTG-loaded PLGA NPs (lipids@PL)
58 with different surface coatings using a microfluidic chip. (Scheme 1). PLGA was
59 dissolved in DMF and TFE (v/v = 7:3) to form a 10 mg/mL PLGA solution. The
60 initial concentration of LTG in PLGA solution was 238 $\mu\text{g/mL}$. For lipids@PL, the
61 lipid solution was composed of DPPC, cholesterol, DSPE-PEG with a molar ratio of
62 80:16:11, For D-T7-lipids@PL, the lipid solution was composed of DPPC,
63 cholesterol, DSPE-PEG2k, DSPE-PEG2k-D-T7 with a molar ratio of 80:16:9:2. For
64 preparing Tet1-lipids@PL, the lipid solution was composed of DPPC, cholesterol,
65 DSPE-PEG2k, DSPE-PEG2k-Tet1 with a molar ratio of 80:16:9:2. For preparing D-
66 T7/Tet1-lipids@PL NPs with different D-T7/Tet1 ratios (2:1, 1:1, and 1:2), the lipid
67 solutions were composed of DPPC, cholesterol, DSPE-PEG2k, DSPE-PEG2k-D-T7
68 and DSPE-PEG2k-Tet1 with a molar ratio of 80:16:8:2:1, 80:16:8:1:1, and
69 80:16:8:1:2 respectively. The synthesis process of the nanoparticles on the
70 microfluidic channels is shown in Scheme 1. The flow rate of PLGA and lipids was 3
71 mL/h, and the flow rate of H₂O was 120 mL/h.

72 The microfluidic chip was composed of two parts. The first part of the chip was
73 composed of three inlets and a straight synthesis channel which was divided into two
74 curved channels to symmetrically connect the central inlet of the second part. The
75 mixed solution of PLGA and LTG flowed into the central inlet and was precipitated in
76 the water flowing from the flanking inlets to form a hydrophobic PLGA@LTG (PL)
77 core in the first part. In the second part, a central inlet connected to the two curved
78 channels from the first part and formed a single channel which extended and formed a
79 double spiral channel connecting to an outlet. In the second part, through the
80 hydrophobic attraction between the tail end of the lipids and the PLGA, the lipid
81 monolayer shell was assembled on the surface of the PL core to synthesize lipids@PL.
82 Targeting peptides conjugated to DSPE-PEG2k including D-T7-DSPE-PEG2k, and
83 Tet1-DSPE-PEG2k mixed with the lipids at certain ratios were introduced into the
84 central inlet of the second part to form lipids@PL nanoparticles with different

85 targeting molecules. In addition, we also synthesized D-T7/Tet1-lipids@PL NPs
86 using conventional methods.³

87 Dynamic light scattering (DLS, Zetasizer 3000HS) and transmission electron
88 microscopy (TEM, HT-7700) were used to characterize the morphology, size and size
89 distribution, and surface charge of the nanoparticles. Each sample was tested three
90 times separately. The samples for TEM were diluted and negatively stained with 2%
91 uranyl acetate.

92 **Encapsulation efficiency of LTG by D-T7/Tet1-lipids@PL NPs**

93 To determine the encapsulation efficiency of LTG by D-T7/Tet1-lipids@PL NPs, we
94 prepared different concentrations of LTG (0, 0.3125, 0.625, 1.25, 2.5, 5, 10, 20, 40,
95 80 µg/mL), and established the standard curve of LTG concentration by a UV-VIS
96 spectrophotometer (UV-2600 Shimadzu) with the excitation wavelength at 306 nm.
97 The D-T7/Tet1-lipids@PL NPs were filtered by a microsep (MWCO=10 KD,
98 Millipore) after synthesized by the microfluidics. The concentration of LTG in the
99 NPs was determined by the UV spectrophotometer.

100 **LTG release from the D-T7/Tet1-lipids@PL NPs**

101 To study the release of LTG in various conditions, the free LTG and D-T7/Tet1-
102 lipids@PL(2:1) NPs (238 µg/mL LTG) were added to dialysis bags (MW=3 KD,
103 Millipore). The bags were placed into PBS (pH=7.2, 3 mL), followed by an
104 incubation for 72 h on a shaking table at 37°C. We collected the dialysate at each
105 predetermined time point (0, 3, 6, 9, 24, 48, 72 h), and moved the dialysis bags into
106 fresh PBS (3 mL). The concentration of LTG was determined using a UV
107 spectrophotometer with the excitation wavelength at 306 nm. The cumulative release
108 rate at each time point was calculated according to the formula: release rate at time i
109 (%) = (sum of LTG concentration before i) / (sum of LTG concentration at 72 h)
110 $\times 100\%$.

111 **Quantification of encapsulation efficiency of DSPE-PEG-D-T7 and DSPE-PEG-**
112 **Tet1 in D-T7/Tet1-lipids@PL NPs**

113 To quantitatively determine the encapsulation efficiency of DSPE-PEG-D-T7 and
114 DSPE-PEG-Tet1 in the D-T7/Tet1-lipids@PL NPs, we labeled D-T7 peptide and
115 Tet1 peptide with rhodamine B (RHB) and FITC respectively. We prepared different
116 concentrations of LTG (0, 2.5, 5, 10, 50, 100, 200 µg/mL), and established the
117 standard curve of D-T7-RHB and Tet1-FITC concentrations by a UV-vis
118 spectrophotometer (UV-2600 Shimadzu) with the excitation wavelength at 554 nm
119 and 488 nm, respectively. The D-T7/Tet1-lipids@PL NPs were filtered by a microsep
120 (MWCO=10 KD, Millipore) after synthesized by the microfluidics. The concentration
121 of D-T7 and Tet1 in the NPs was determined by the UV-vis spectrophotometer.

122 **Cells and animals**

123 Human neuroblastoma cells (SH-SY5Y) were from Kunming Cell Bank. Mouse
124 cerebrovascular endothelioma cells (bEnd.3, KG593) were from Shenzhen Btek
125 Technology Co., LTD. For cell culture, SH-SY5Y cells were cultured in RPMI 1640
126 medium (15-20 % FBS, 1% penicillin/streptomycin). bEnd.3 cells were cultured in
127 DMEM (10 % FBS, 1% penicillin/streptomycin). For primary culture of hippocampal
128 neurons, the neonatal rats of 0-3 days were decapitated.⁴ The brain was taken out and
129 placed in pre-cooled PBS. The hippocampus was extracted and digested by 0.25%
130 trypsin in a 37 °C water bath for 15 min. The dissociated neurons were inoculated in
131 confocal dishes or 12-well plate with DMEM/F12 medium (10 % FBS, 1 %
132 penicillin/streptomycin). After the cells adhered to the wall, the F12 medium was
133 replaced with the neurobasal medium (2 % B27, 1 % penicillin/streptomycin). The
134 medium was changed every three days.

135 All protocols of animal experiments are approved by the Institutional Animal Care
136 and Use Committee at the Southern University of Science and Technology (resolution
137 number: SUSTC-JY2020124). All animals including male BALB/c nude mice and

138 male/female C57BL/6 mice (6-8 weeks) and neonatal rats were from Guangdong
139 Medical Laboratory Animal Center (Guangzhou, China).

140 **Cellular internalization**

141 For cellular uptake study, hippocampal neurons, bEnd.3 cells and SY5Y cells were
142 seeded into the confocal dishes with a density of 1×10^5 cells per dish, followed by the
143 addition of DiI-labelled nanoparticles. After co-incubation for 6 h at 37°C, the cells
144 were rinsed with pre-warmed PBS three times, and were fixed with 4% PFA for 15
145 min at 37°C. The cells were treated with PBS three times for 5 min each. The nuclei
146 were stained with DAPI for 10 min. The neurons were visualized by staining the
147 tubulin, whereas the SY5Y cells were visualized by staining the phalloidin. After
148 washing with PBS three times for 5 min each, we imaged the cells using a confocal
149 laser scanning microscopy (CLSM, A1, Nikon).

150 Uptake of DiI-labelled nanoparticles by hippocampal neurons, bEnd.3 cells and
151 SY5Y cells was quantified by a flow cytometry (FACScanto, BD Biosciences). The
152 hippocampal neurons, bEnd.3 cells and SY5Y cells were seeded in twelve-well plates
153 with a density of 1×10^5 cells per well. The cells were treated with DiI-labelled
154 nanoparticles for 6 h. The cells were washed with pre-warmed PBS three times, and
155 collected after trypsin treatment. Cells were quantitatively analyzed by the flow
156 cytometry.

157 **Penetration experiment of D-T7/Tet1-lipids@PL NPs in *in vitro* BBB model**

158 The hippocampal neurons were seeded into the lower chamber Transwell (Corning)
159 with a density of 5×10^4 cells per dish, and the bEnd.3 cells were seeded on 8.0 μm PC
160 membrane with a density of 1×10^5 cells. The penetration experiment of nanoparticles
161 started after the transendothelial electrical resistance (TEER) reached a stable state of
162 about 80 Ω . After co-cultivating various nanoparticles in the BBB model for 6 hours,
163 we rinsed the neurons three times with pre-warmed PBS, and collected the cells after
164 trypsin treatment. The cells were quantitatively analyzed by the flow cytometry.

165 ***In vivo* fluorescence imaging**

166 In order to explore the transcytosis ability and accumulation capacity of the BBB,
167 living fluorescence imaging technology (IVIS Spectrum, PerkinElmer) was used to
168 monitor the biodistribution of a near infrared (NIR) dye (DiR)-labelled nanoparticles
169 in nude mice. IVIS® Lumina Series III Imaging System can be used in two modes:
170 bioluminescence and fluorescence. We used the fluorescence mode in this study. The
171 focal length of the lens was 50 mm, and the light transmittance was 95%. The field of
172 view ranged from 5×5 cm to 12.5×12.5 cm. The lens size of the charge coupled
173 device (CCD) was 13.3×13.3 mm with a 1 million pixel. The imaging parameters we
174 set were: the field of view was 12.5×12.5 cm; the wavelength of excitation filter was
175 740 nm, the wavelength of emission filter was 790 nm; the binning factor was 4; the
176 luminescent exposure time was 0.5s; the subject height was 1.5cm; the f number was
177 2. The maximum excitation wavelength and emission wavelength of DiR was 748 nm
178 and 780 nm respectively. The nude mice were injected with DiR-labelled
179 nanoparticles (DiR=0.75 mg/mL) *via* tail vein, respectively. Fluorescence images
180 were obtained at 0.5, 2, 4, 6, 12, and 24 h. We selected the brain and the whole body
181 ROIs respectively, and measured the corresponding fluorescence intensity. The mice
182 were sacrificed 24 h after the injection, and their organs were collected and imaged by
183 using the *in vivo* imaging system.

184 **Immunohistochemistry**

185 PBS and various DiI-labelled D-T7/Tet1-lipids@ PL were injected to seven groups of
186 C57BL/6 mice (n = 3) *via* tail vein. The mice were sacrificed 6 h later. After
187 perfusion, the brain tissue was removed and immersed in paraformaldehyde (4% w/v).
188 A Leica CM1950 cryostat microtome was used to slice the brain into 35-µm thick
189 coronal slices. The slices were treated with PBS three times for 5 min each and
190 blocked in 10% normal goat serum for 1 h. The samples were then incubated with
191 primary antibodies (GFAP; NeuN) overnight at room temperature, washed with PBS
192 and incubated with secondary antibodies (Alexa Fluor 594-conjugated affinpure goat

193 anti-rabbit IgG (H_βL); Alexa Fluor 488 affinpure goat anti-rabbit IgG (H_βL) for 1 h.
194 After washing with PBS three times for 5 min each, the sections were mounted onto
195 gelatin-coated slides and cover slipped with a signal enhancer (ProLong Gold
196 Antifade Reagent with DAPI). In addition, we performed immunofluorescence
197 staining of blood vessels in the D-T7/Tet1-lipids@PL(2:1)-treated brains using CD31
198 antibody. The mounted slices were observed and imaged using an Olympus slide
199 scanner (VS120).

200 **Cytotoxicity assay**

201 The cytotoxicity of various lipids@PL nanoparticles was assessed by CCK-8 assay.
202 The hippocampal neurons and SY5Y cells were seeded into 96-well plates with a
203 density of 5×10^4 cells per well in the neurobasal medium for 24 h prior to the
204 experiment. The culture medium was substituted with 100 μ L lipids@PL with
205 different surface modification ligands with serial concentrations from 62.5 μ g/mL to
206 1000 μ g/mL for 24 h. Each concentration was replicated in 5 wells. the medium in
207 each well was replaced with freshly medium with 1% CCK-8 for 1 h. the absorbance
208 was measured by a microplate reader (Spark, Tecan) at 450 nm.

209 We used cell viability assay kit to characterize cytotoxicity. Neurons were seeded
210 into confocal dishes with a density of 1×10^5 cells per dish, 100 μ L lipids@PL
211 nanoparticles with different surface modification ligands (1000 μ g/mL) were added.
212 After co-incubation for 24 h at 37 °C, the cells were washed with pre-warmed PBS
213 two times, cell viability assay kit was used to characterize the toxicity of the
214 nanoparticles to the neurons, and the cells were imaged using a confocal microscopy.

215 **Hemolysis test**

216 Mouse whole blood was collected in a heparin-treated centrifuge tube and diluted
217 with PBS. The diluted blood was centrifuged at 2000 rpm for 5 min and the
218 supernatant was removed. The red blood cells were suspended in PBS (pH 7.4) at a
219 final concentration of 2 %. Subsequently, the cell suspension was incubated with

220 purified water (positive control), PBS (negative control) and nanoparticles of different
221 concentrations (62.5, 250, and 1000 µg/mL) at 37 °C for 4 h. The red blood cells were
222 centrifuged at 2000 rpm for 5 min, and 100 µL supernatant was transferred to a 96-
223 well plate. The sample was measured at 490 nm with a microplate reader (Spark,
224 Tecan).

225 ***In vivo* electrophysiological recording for KA-induced acute epilepsy model**

226 For the construction of KA-initiated epilepsy model, C57BL/6J mouse was
227 anesthetized with urethane (1.5 g/kg), and the head was fixed in a standard stereotaxic
228 frame (RWD). The cranium was exposed through a small midline scalp incision.
229 Holes were drilled through the skull, and a drug delivery electrode array was directed
230 towards the brain at the following stereotaxic coordinates: the electrode tip at
231 anteroposterior (AP) -2.06 mm, mediolateral (ML) -1.35 mm and dorsoventral (DV) -
232 2.10 mm for recording in the dorsal hippocampus (dHPC); The silica tubing at AP -
233 2.06 mm, ML -1.80 mm and DV -1.60mm for drug delivery in the dorsal
234 hippocampus. KA (0.3 mg/mL in PBS solution) was unilaterally injected into the
235 dorsal hippocampus via the drug delivery electrode array using a micropump.

236 Electrophysiological recordings were performed with a 64-channel neural
237 acquisition processor (Plexon). The local field potentials (LFPs) were sampled at 1
238 kHz, and bandpass was filtered at 1-500 Hz. Neural signal analyses were performed
239 using a Plexon NeuroExplorer software and a custom-designed Matlab (Mathworks)
240 code. Phosphate-buffered saline (PBS), LTG (2 mg/kg), lipids@PL (2 mg/kg), Tet1-
241 lipids@PL (2 mg/kg), D-T7-lipids@PL (2 mg/kg), D-T7/Tet1-lipids@PL (2:1) (2
242 mg/kg) and D-T7/Tet1-lipids@PL (2:1) (5 mg/kg) were intravenously injected 2 h
243 before the establishment of the KA model. LFPs were monitored and recorded in the
244 dorsal hippocampus of the mice after KA injection, and the signals were recorded for
245 2.5 h by the neural acquisition processor.

246 ***In vivo* behavior recording for pilocarpine-induced acute epilepsy model**

247 For the construction of pilocarpine-initiated epilepsy model, C57BL/6 mice were
248 divided into 4 groups, and injected intraperitoneally with methylscopolamine (1
249 mg/kg). 30 min later, pilocarpine (320 mg/kg) was intraperitoneally injected.
250 Approximately 10 min after the administration, persistent seizures were induced. We
251 injected PBS, lipids@PL (2 mg/kg), and D-T7/Tet1-lipids@PL(2:1) (2 mg/kg)
252 intravenously respectively 2 h before the construction of the model. We recorded the
253 real-time epileptic behavior for 40 min, 1.5 h, and 4 h by video.

254 **Treatment of D-T7/Tet1-lipids@PL NPs in a KA-induced chronic epilepsy model**

255 C57 BL/6J mice of 6-8 weeks were used for constructing chronic epilepsy models.
256 KA (0.3 mg/mL, 550 nL) was injected into the right dorsal hippocampus (AP -2.06
257 mm, ML -1.80 mm, DV -1.80 mm) *via* a 33-gauge metal needle connected with a
258 micro-syringe pump (UMP3/Micor4). Electrophysiological recordings and
259 immunohistochemistry were performed in epileptic mice treated with PBS, LTG, D-
260 T7/Tet1-lipids@PL(2:1) NPs for 6 weeks.

261 **Safety evaluation**

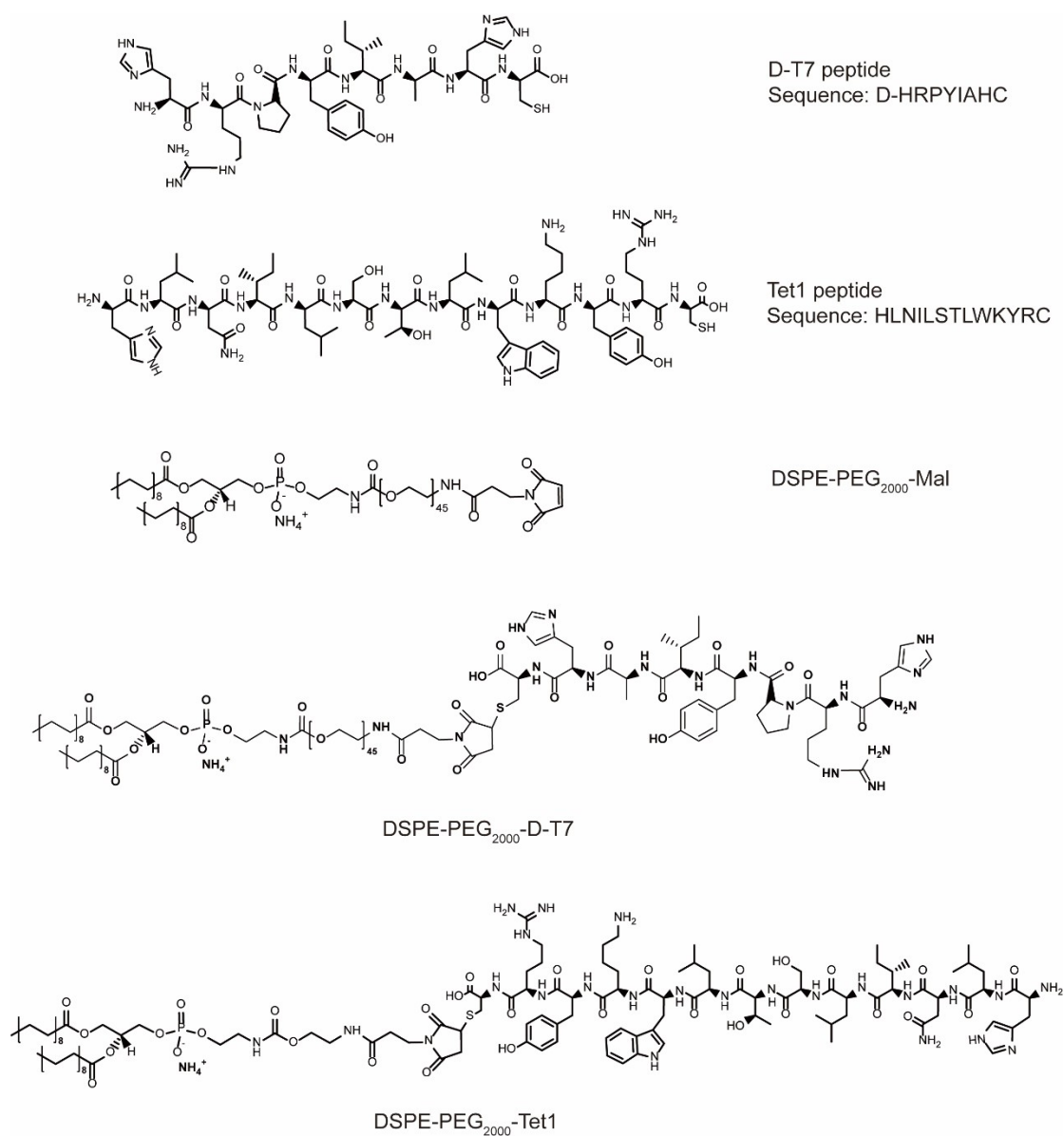
262 After the experiment, the mice were sacrificed and dissected, and the heart, liver,
263 spleen, lung, kidney, and brain were sliced for hematoxylin-eosin (H&E) staining. In
264 addition to H&E staining, blood biochemical indicators markers were evaluated. We
265 took 500 μ L of blood from the eyeball, at 3500 rpm, 4°C, centrifuged for 5 min, took
266 out 100 μ L of serum and used the automatic biochemical analyzer (MS-480) to test
267 the blood biochemical indicators. The parameters tested in this study included
268 glutamic-pyruvic transaminase (ALT), glutamic oxalacetic transaminase (AST),
269 (alkaline phosphatase) ALP, total protein (TP), serum albumin (ALB), carbamide
270 (urea). Similarly, take 100 μ L of whole blood from the eyeball for routine blood
271 testing. The parameters tested in this study included white blood cells (WBC), red
272 blood cell (RBC), hemoglobin (HGB), mean RBC hemoglobin (MCH), red cell

273 distribution width (RDW), platelets (PLT), mean platelet volume (MPV), mean
274 corpuscular hemoglobin concentration (MCHC) and mean corpuscular volume (MCV).

275 Statistics

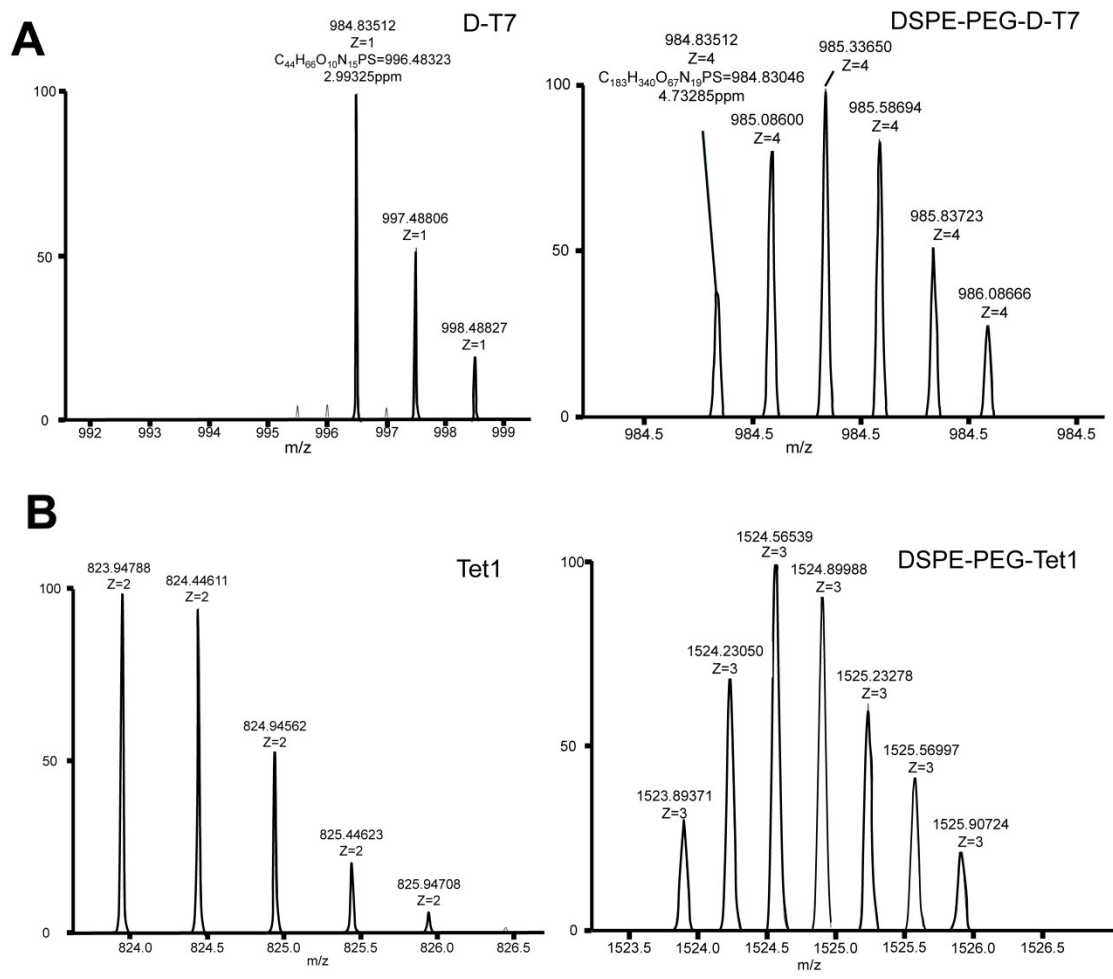
276 The data were expressed as mean \pm SD. The statistical analysis of different
277 experimental groups was performed using Student's *t* test. $P < 0.05$, $P < 0.01$, $P < 0.001$
278 were used as the standards of statistical significance.

279 Results and Discussion



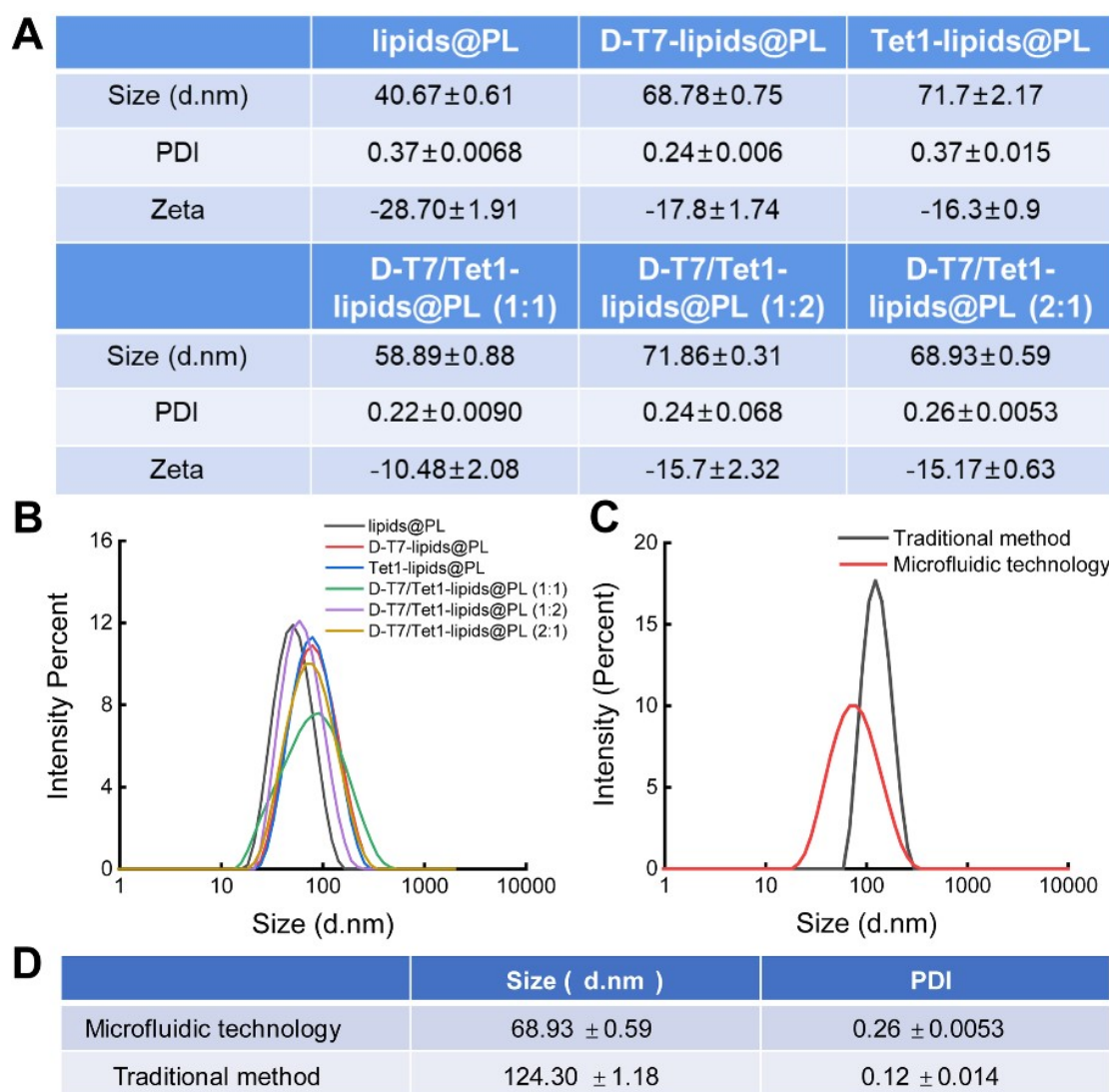
280

281 **Figure S1** Structural formula of the peptides and the DSPE-PEG-peptides.



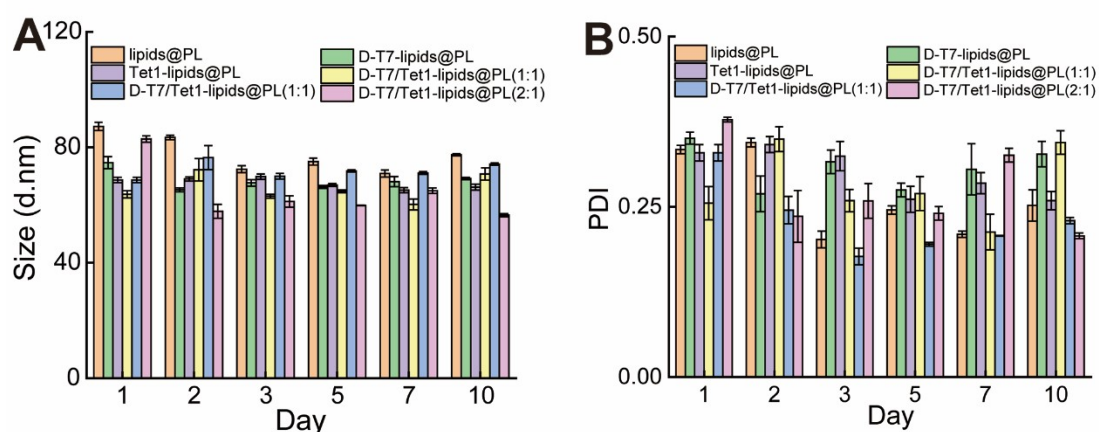
282

283 **Figure S2** Mass spectra of DSPE-PEG-peptides. (A) Mass spectra of D-T7 and
 284 DSPE-PEG-D-T7. (B) Mass spectra of Tet1 and DSPE-PEG-Tet1.



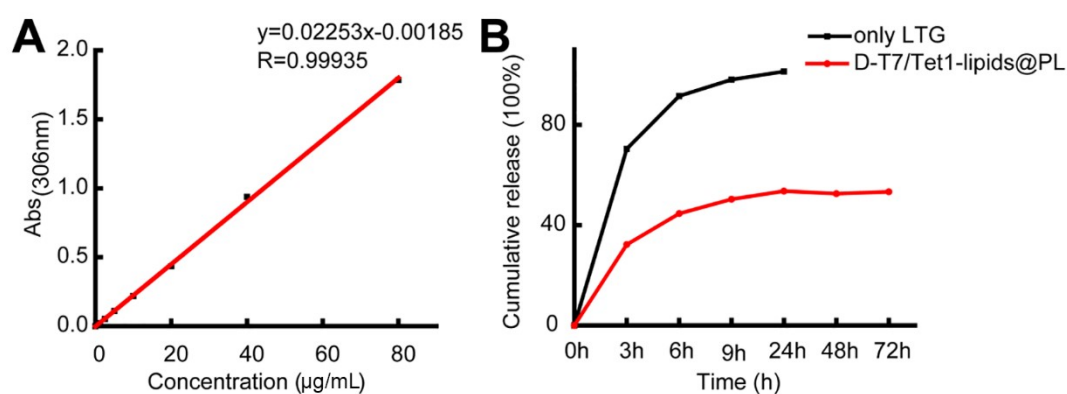
285

286 **Figure S3** Characterization of various nanoparticles. (A-B) DLS characterization of
 287 D-T7-Lipids@PL, Tet1-Lipids@PL, and D-T7/Tet1-Lipids@PL with different D-
 288 T7/Tet1 ratios (1:2, 1:1, and 2:1). (C-D) DLS characterization of D-T7/Tet1-
 289 lipids@PL(2:1) synthesized by microfluidic chip and traditional method.



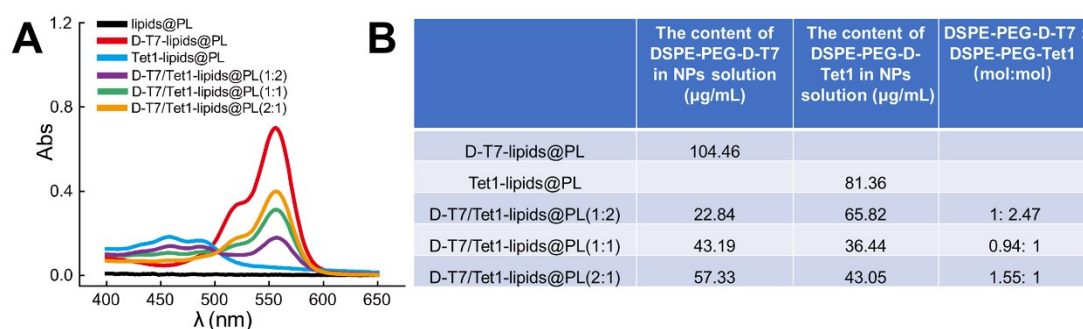
290

291 **Figure S4** Stability test of various nanoparticles in 10 days characterized by DLS.



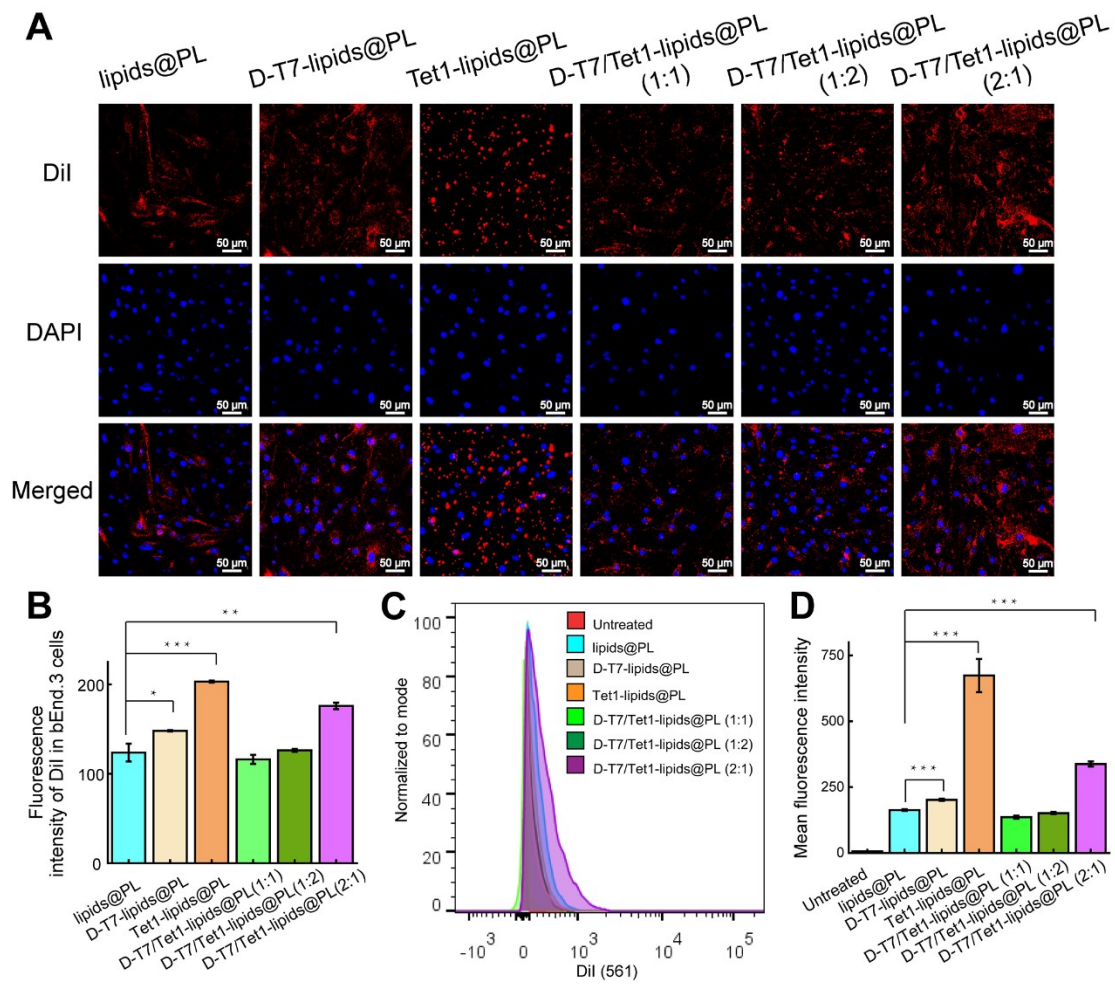
292

293 **Figure S5** Drug release test of D-T7/Tet1-lipids@PL(2:1) NPs. (A) The standard
294 curve of LTG absorbance at 360 nm. (B) Cumulative drug release of D-T7/Tet1-
295 lipids@PL(2:1) NPs in PBS (pH 7.4).



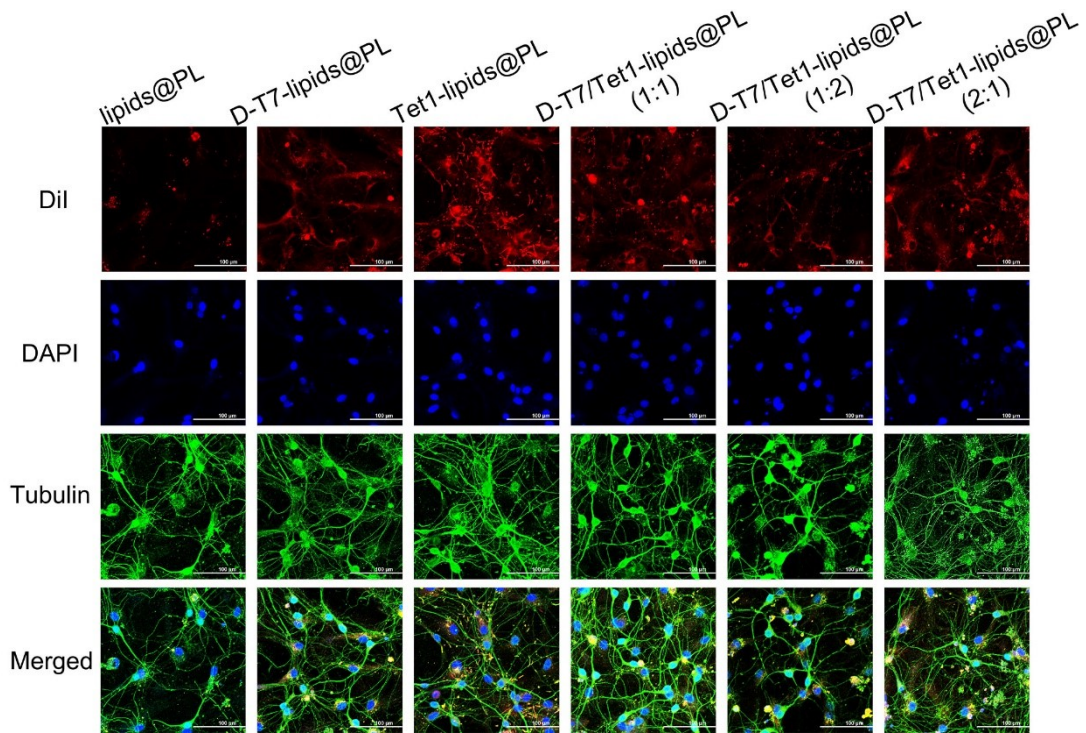
296

297 **Figure S6** UV-vis spectra to characterize the DSPE-PEG-D-T7 and DSPE-PEG-Tet1
298 in various nanoparticles. A) UV-vis spectra of various NPs. B) The quantified data of
299 each NP based on the UV-vis spectra.

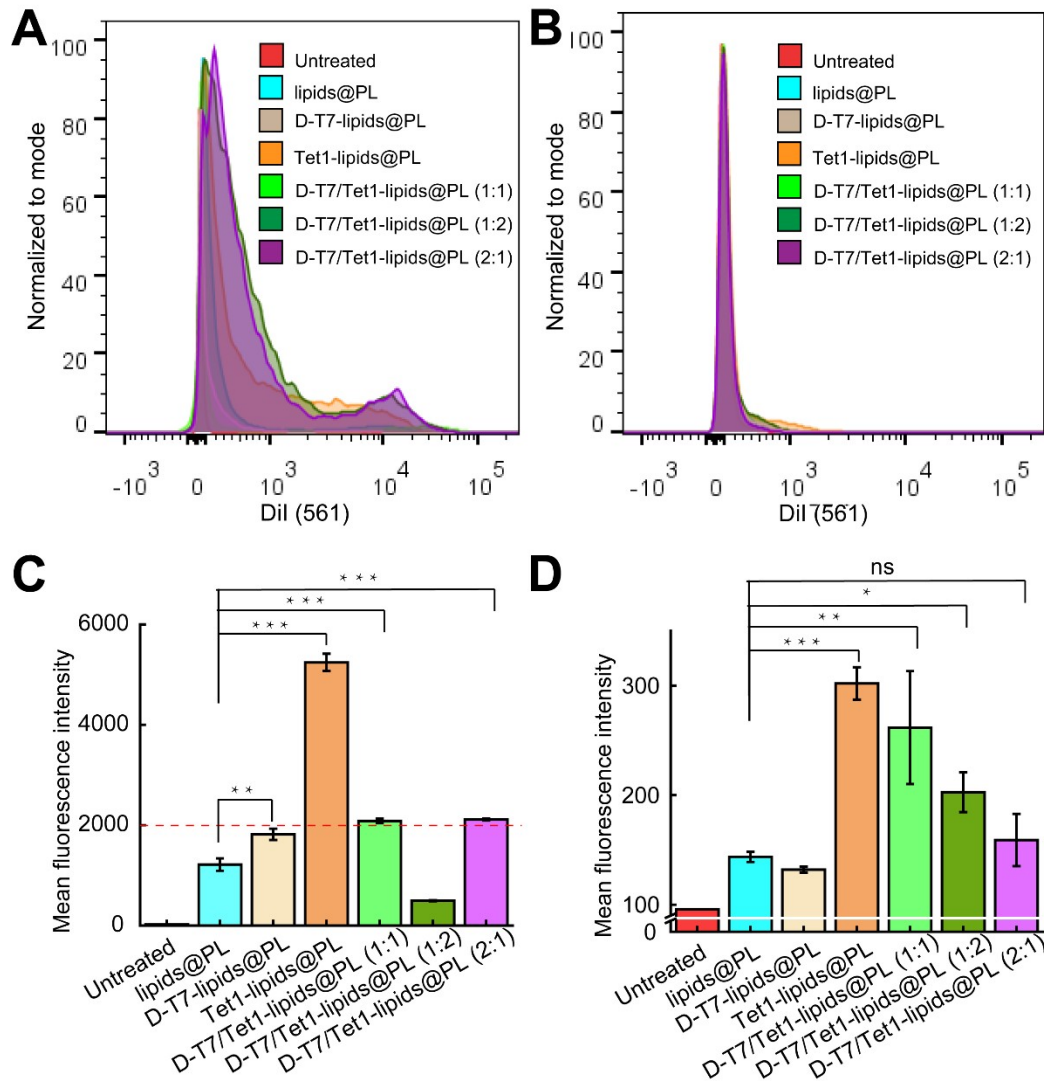


300

301 **Figure S7** *In vitro* uptake of various NPs with different D-T7/Tet1 concentration
 302 titrations by bEnd.3 cells. (A) Confocal microscopy images of bEnd.3 cells incubated
 303 with various nanoparticles at 37 °C for 6 h. The nanoparticles are labeled by DiI.
 304 Nuclei are stained by DAPI (blue). Scale bars, 50 μm. (B) Quantitative analysis of the
 305 confocal fluorescence images of the nanoparticles internalized in the bEnd.3 cells
 306 using Image J. (C) Flow cytometry histogram of bEnd.3 cells incubated with various
 307 nanoparticles at 37 °C for 6 h. DiI is used to label the nanoparticles. (D) Data from the
 308 flow cytometry which shows the mean fluorescence intensity of the bEnd.3 cells
 309 incubated with various nanoparticles at 37 °C for 6 h. The nanoparticles are labelled
 310 by DiI. * $P < 0.005$, *** $P < 0.001$.

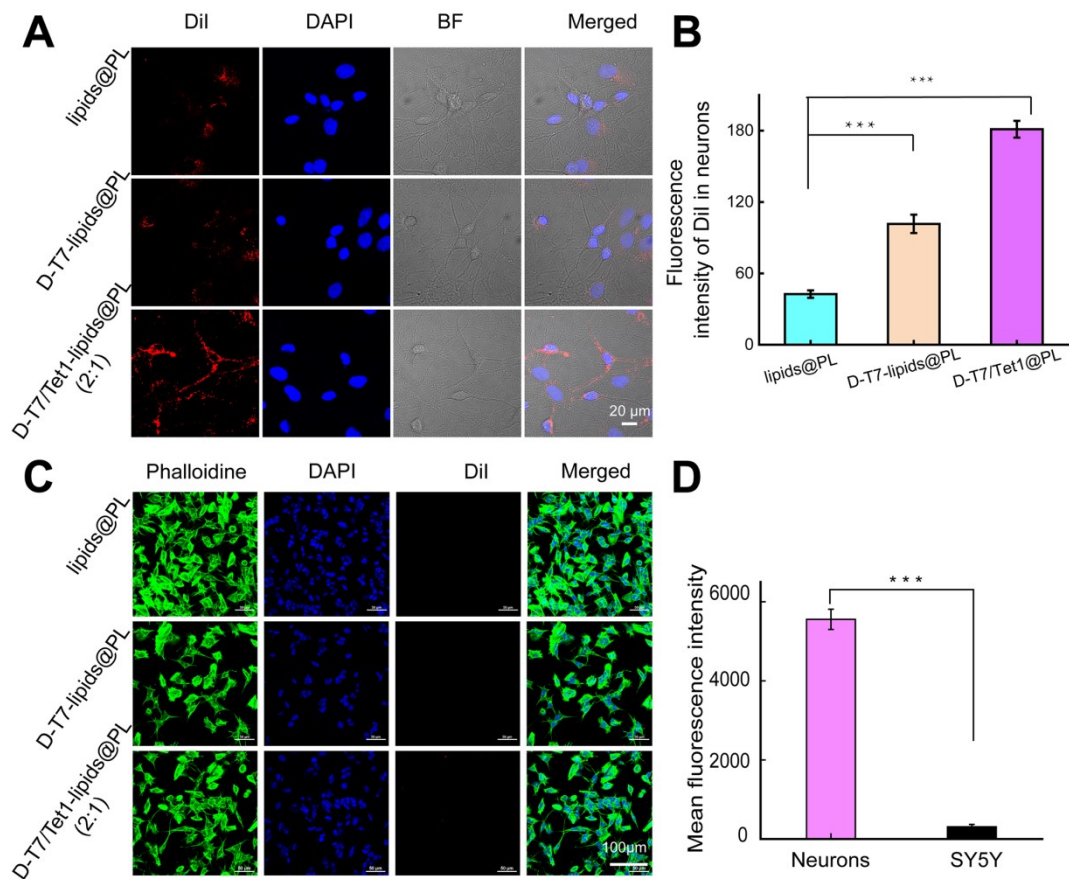


312 **Figure S8** Confocal microscopy images of neurons incubated with various
 313 nanoparticles at 37 °C for 6 h. The nanoparticles were labeled by DiI. The nuclei were
 314 stained by DAPI (blue). The neurons were stained by tubulin (Green). Scale bars, 100
 315 µm.



316

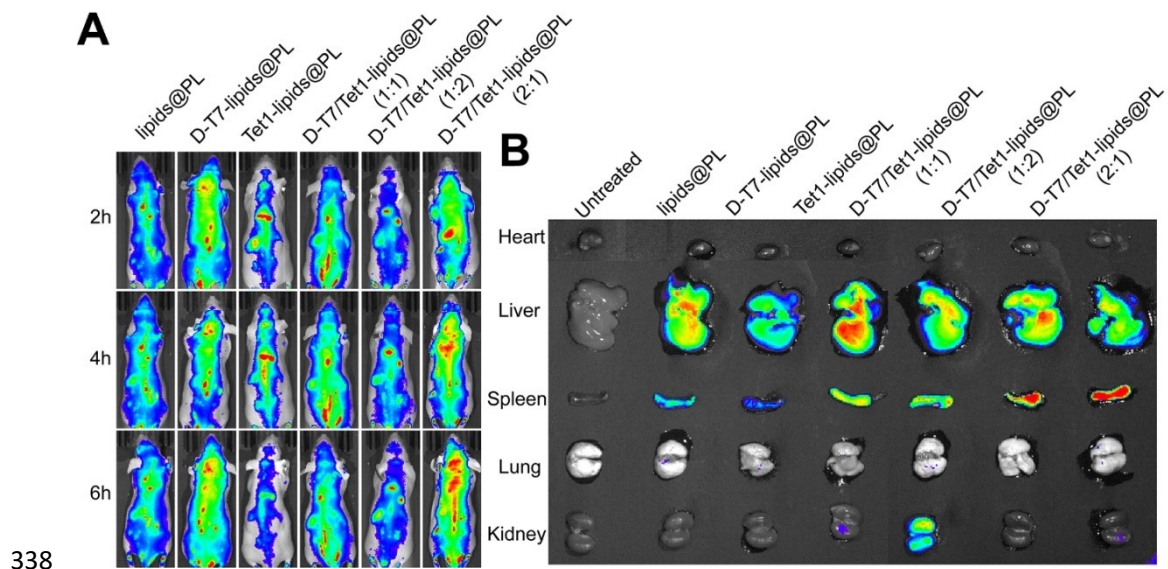
317 **Figure S9** *In vitro* internalization of various NPs with different D-T7/Tet1
 318 concentration titrations in hippocampal neurons and SY5Y cells. Flow cytometry
 319 histogram of hippocampal neurons A) and SY5Y cells B) incubated with
 320 nanoparticles at 37 °C for 6 h. DiI is used to label the nanoparticles. Data from flow
 321 cytometry show the mean fluorescence intensity of the hippocampal neurons C) and
 322 SY5Y cells D) incubated with nanoparticles at 37 °C for 6 h. * $P < 0.05$, ** $P < 0.01$,
 323 *** $P < 0.001$.



324

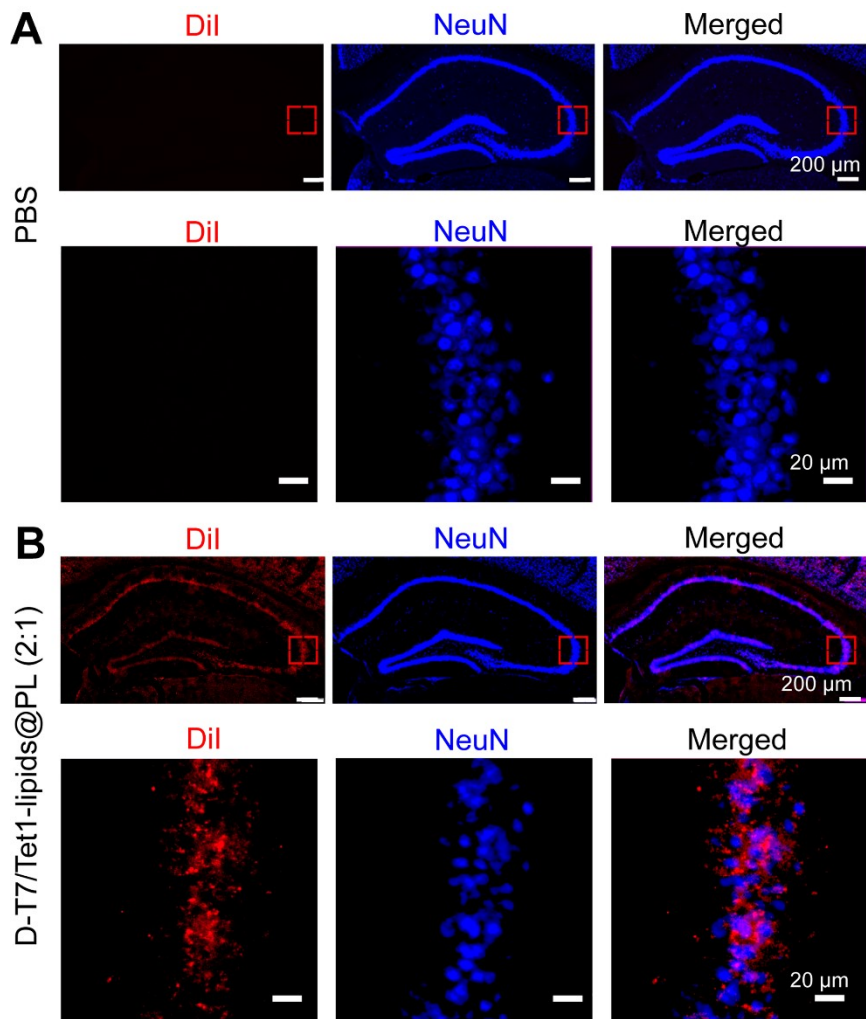
325 **Figure S10** *In vitro* internalization of NPs by hippocampal neurons and SY5Y cells.
 326 (A) Confocal microscopy images of hippocampal neurons incubated with lipids@PL,
 327 D-T7-lipids@PL, and D-T7/Tet1-lipids@PL (2:1) at 37 °C for 6 h. The nanoparticles
 328 are labeled by DiI. The cell nuclei are stained by DAPI (blue). Scale bars, 20 μm. (B)
 329 Quantitative analysis of the fluorescence of the nanoparticles internalized in the
 330 hippocampal neurons using Image J. (C) Confocal microscopy images of the SY5Y
 331 cells incubated with various nanoparticles at 37 °C for 6 h. The nanoparticles are
 332 labeled by DiI. The cell nuclei are stained by DAPI (blue). The SY5Y cells are
 333 stained by phalloidin (green). Scale bars, 100 μm. (D) Data from flow cytometry
 334 which shows the mean fluorescence intensity of the hippocampal neurons and SY5Y
 335 cells incubated with the nanoparticles at 37 °C for 6 h. The nanoparticles are labelled
 336 by DiI. *** $P < 0.001$.

337



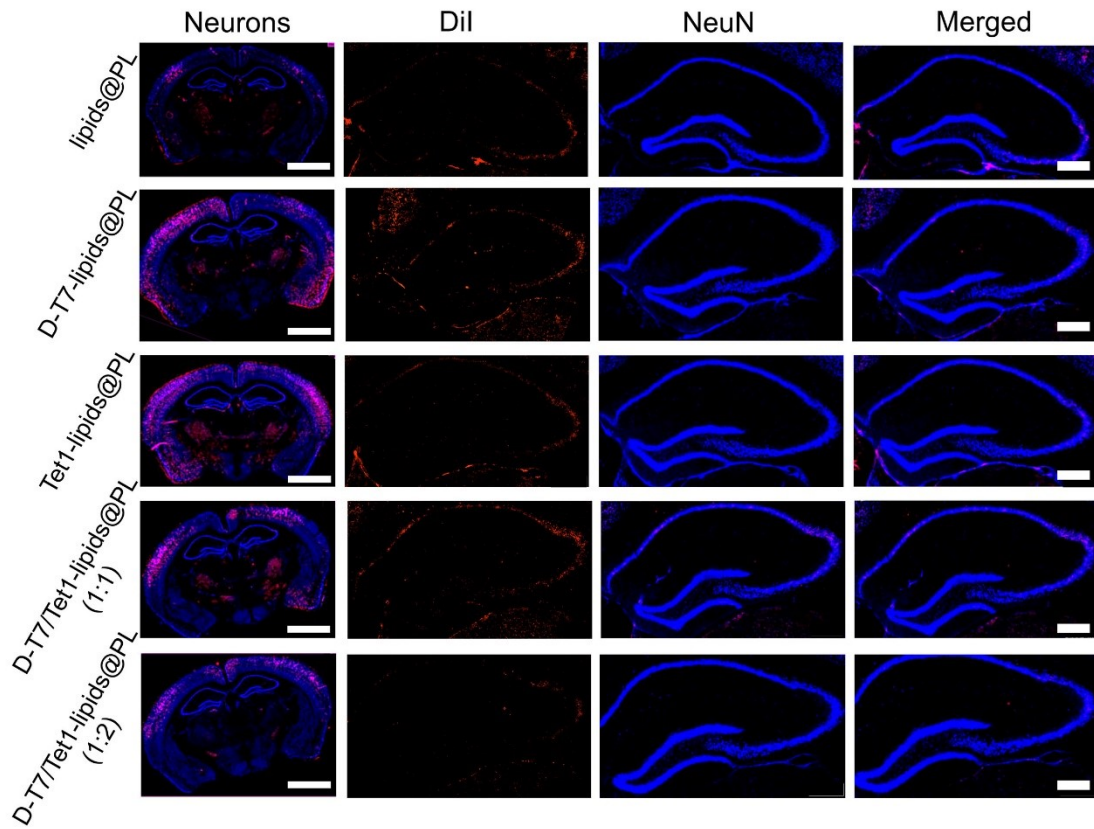
339 **Figure S11** Fluorescence distribution of different NPs *in vivo*. (A) *In vivo* imaging
 340 shows the distribution of different NPs with different D-T7/Tet1 concentration
 341 titrations in mice at different time points. (B) Fluorescent imaging of the organs *ex*
 342 *vivo* 24 h after injection of DiR-labelled NPs.

343

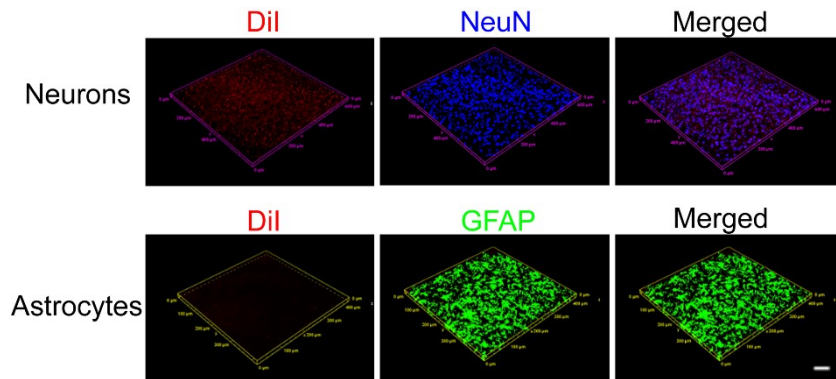


344

345 **Figure S12** Immunofluorescence of mice brain dorsal hippocampus (dHPC) treated
 346 with D-T7/Tet1-lipids@PL(2:1) NPs labelled by DiI. The neuron nuclei are stained
 347 by NeuN (blue). Scale bar, 200 μ m and 20 μ m.

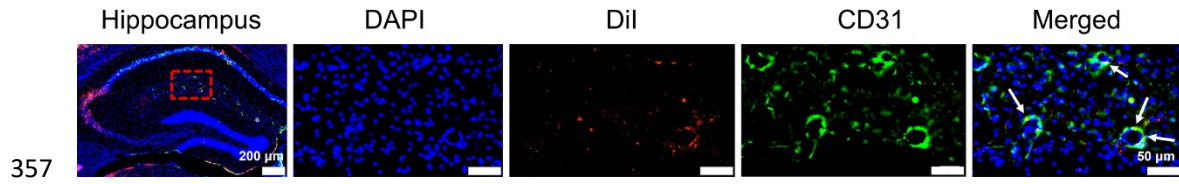


348
 349 **Figure S13** Immunofluorescence of mice brain dorsal hippocampus (dHPC) treated
 350 with various NPs labelled by DiI. The neuron nuclei were stained by NeuN (blue).
 351 Scale bar, 2 mm and 200 μ m.



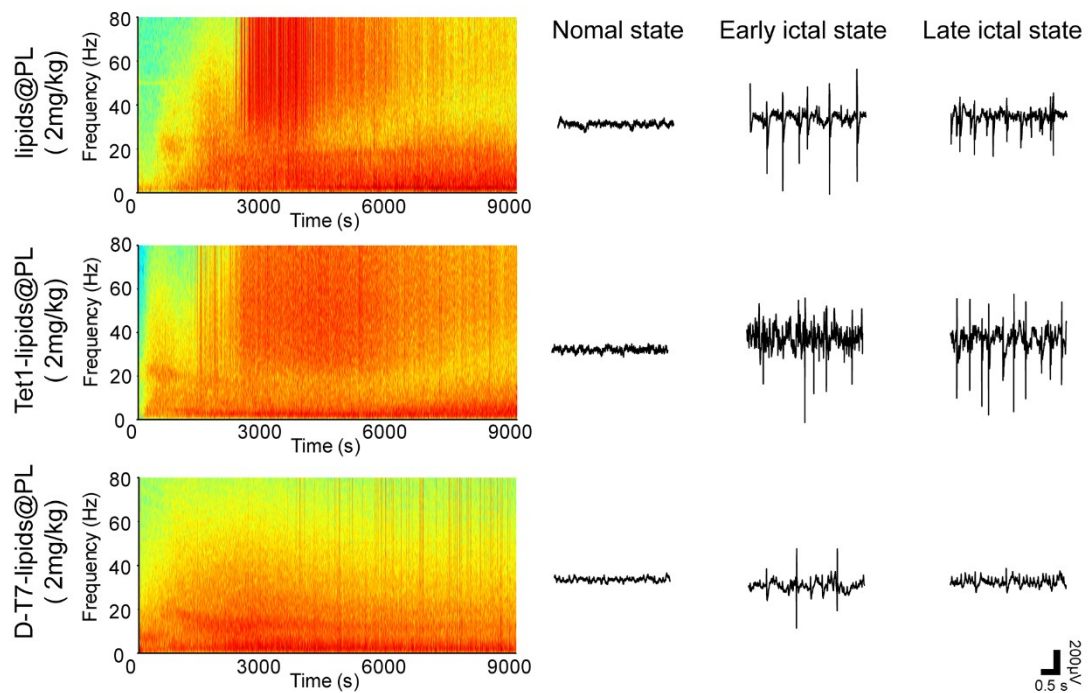
352
 353 **Figure S14** 3D images of immunofluorescence of mice brain treated with D-T7/Tet1-
 354 lipids@PL(2:1) labelled by DiI. The neuron nuclei are stained by NeuN (blue), the
 355 astrocytes are stained by GFAP (green). Scale bar, 100 μ m.

356



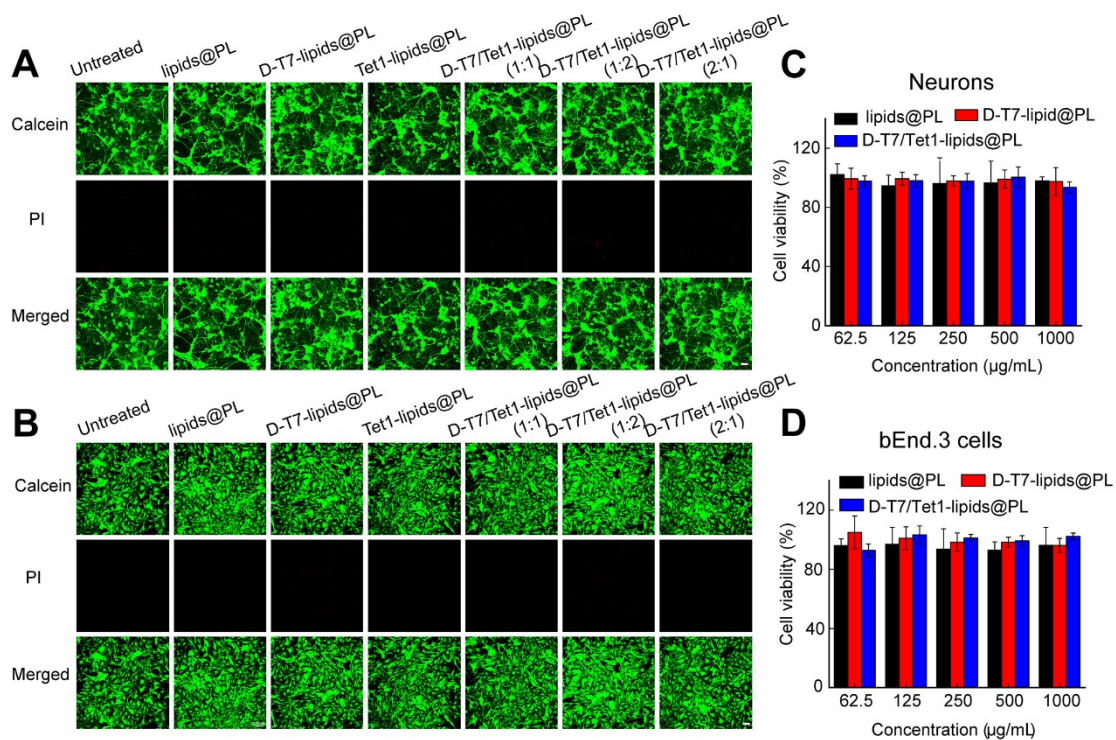
358 **Figure S15** Immunofluorescence of mice brain treated with D-T7/Tet1-
 359 lipids@PL(2:1) NPs labelled by DiI. The cell nuclei were stained by DAPI (blue).
 360 The vascular endothelial cells were stained by CD31 antibody. Scale bar, 200 μm and
 361 50 μm .

362



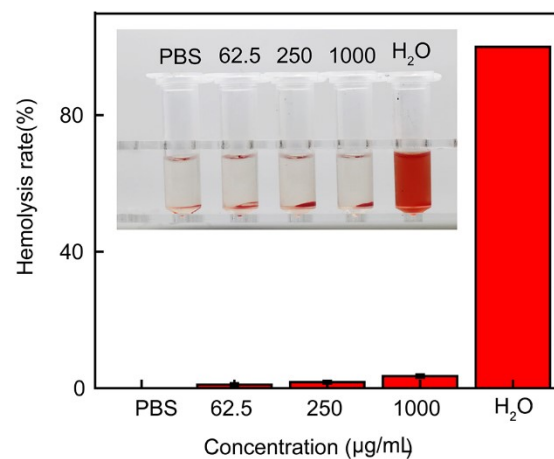
363

364 **Figure S16** A 2.5-hour spectrogram of LFPs recorded in the dorsal hippocampus after
 365 modeling. Raw LFPs are recorded from the representative channels in the dorsal
 366 hippocampus. Representative raw LFPs of normal state, early ictal state and late ictal
 367 state are recorded in the dorsal hippocampus of mice after KA injection.



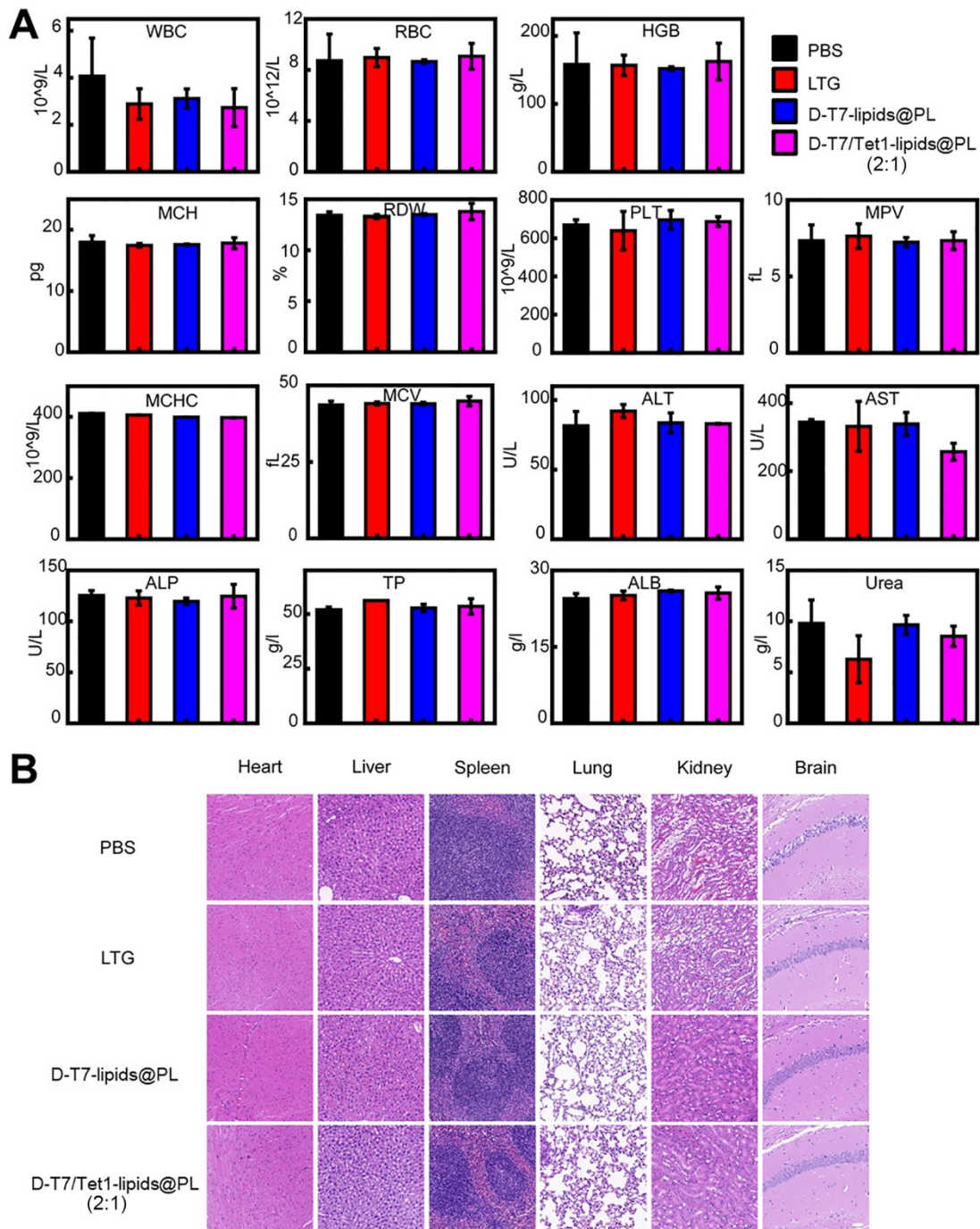
368

369 **Figure S17** Cytotoxicity assay of the nanoparticles. Confocal microscopy image of
 370 hippocampal neurons A) and bEnd.3 cells B) co-cultured with various nanoparticles
 371 for 12 hours. The cells are stained by Calcein (green)/PI (red). Scale bar, 100 µm. The
 372 cell viability of hippocampal neurons C) and bEnd.3 cells D) after 24 h of incubation
 373 with the nanoparticles tested by CCK8 assay.



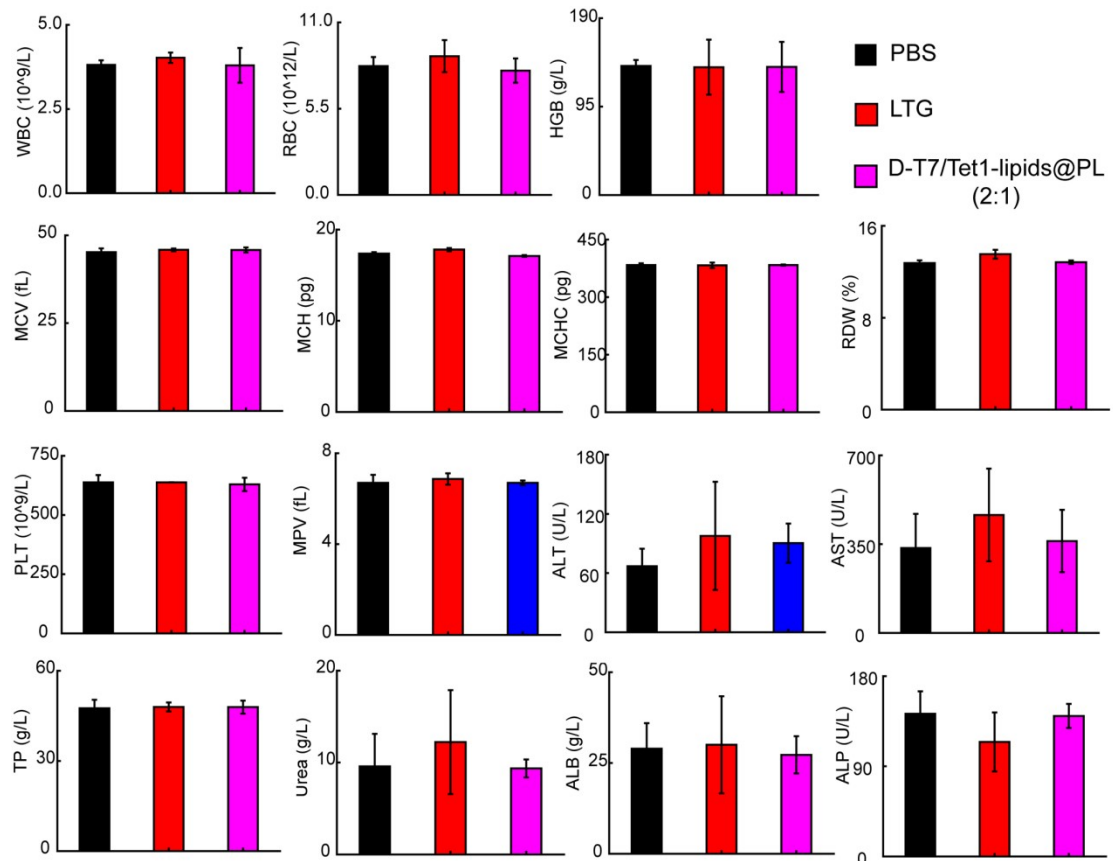
374

375 **Figure S18** Hemolysis test of D-T7/Tet1-lipids@PL (2:1) nanoparticles at different
 376 concentrations. (n = 3).



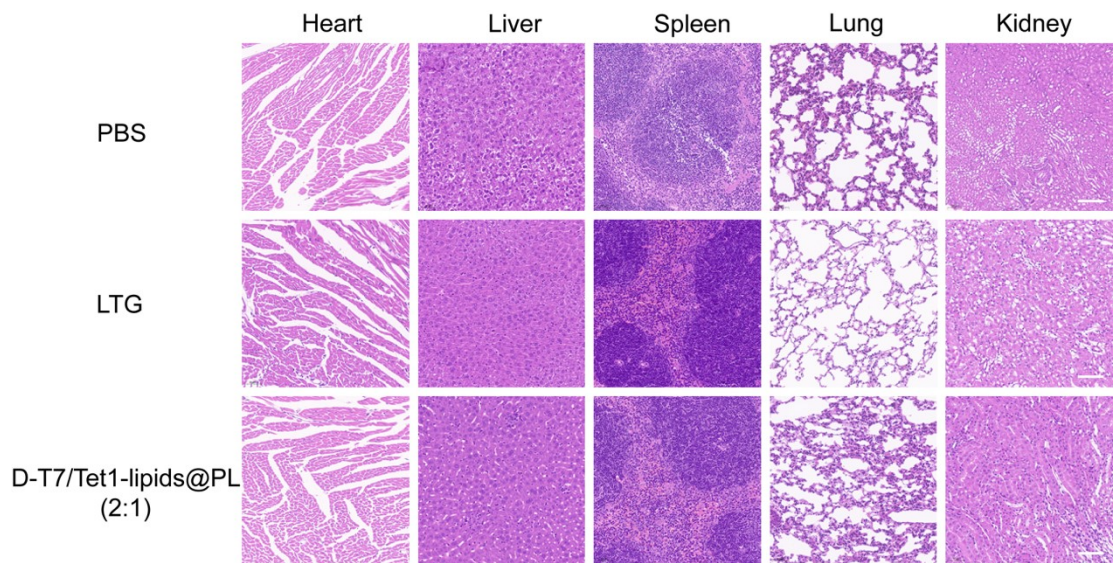
377

378 **Figure S19** Biocompatibility test of various nanoparticles in an acute epilepsy mice
 379 model. (A) *In vivo* biosafety evaluation of various nanoparticles assessed by
 380 hematological markers and biochemical parameters in blood. (B) *In vivo* biosafety of
 381 various nanoparticles assessed by histopathological analysis. Scale bar, 50 μ m. (n = 3).



382

383 **Figure S20** *In vivo* biosafety evaluation of various nanoparticles assessed by
 384 hematological markers and biochemical parameters in blood after 6 weeks of
 385 nanoparticles treatment in a chronic epilepsy model. (n = 3)



386

387 **Figure S21** *In vivo* biosafety of various nanoparticles assessed by histopathological
388 analysis after 6 weeks of nanoparticles treatment in a chronic epilepsy model. Scale
389 bar, 50 μm .

390 **References**

- 391 1 L. Zhang, Q. Feng, J. L. Wang, S. Zhang, B. Q. Ding, Y. J. Wei, M. D. Dong, J.-
392 Y. Ryu, T.-Y. Yoon, X. H. Shi, J. S. Sun, X. Y. Jiang, *ACS Nano*, 2015, **9**, 9912-9921.
- 393 2 Q. Feng, L. Zhang, C. Liu, X. Y. Li, G. Q. Hu, J. S. Sun, X. Y. Jiang,
394 *Biomicrofluidics*, 2015, **9**, 052604.
- 395 3 L. Zhang, J. M. Chan, F. X. Gu, J. W. Rhee, A. Z. Wang, A. F. Radovic-Moreno,
396 F. Alexis, R. Langer, O. C. Farokhzad, *ACS Nano*, 2008, **2**, 1696-1702.
- 397 4 Y. Sun, Z. Huang, W. W. Liu, K. X. Yang, X. Y. Jiang, *Biointerphases*, 2012, **7**,
398 29.
- 399